Supplimentary information on "Climate control on erosion distribution over the Himalaya during past ~100 ka"

1. Litho-Stratigraphy, facies and chronology of the IITK core

The sediment core drilled in IITK site represents an interfluve setting which is situated ~14 km south of the southern bank of the modern Ganga. There is no major sand body in the core (Fig. S1), and since last ~100 ka this site has remained in the interfluve setting. The core does not show any record of major discontinuity. The entire core consists of floodplain facies with continuous over bank muds, intersperse with thin layers of silt (Sinha et al., 2007). The dominant floodplain facies is yellow–brown mud associated with thin silt sheets, the splay deposits. Red–brown mud marks the upper part of each depositional unit. The upper part of the core is interspersed with silt layers. In general, all the individual facies have similar bulk mineralogy (Sinha et al., 2007) with quartz (~65%), mica (20– 25%) and feldspar (10–15%). Texturally, four muddy facies are recognized in this core, with individual facies varying in thickness up to 4 m. Yellow–brown mud, aggradational floodplain sediments, dominates at all locations. Red–brown mud with local silt patches, carbonate nodules and black mottles is the next abundant facies. Hard pale clay, commonly associated with red–brown mud, occurs as rare beds with thickness up to 0.5 m. Carbonate facies consists of layers of carbonate nodules up to 5 cm in diameter, locally termed as 'kankar'. These layers are associated with other facies. There are minor deposits of discrete flooding events at ~35 m and 42.5 m depths. This core consists of two flood plain accretion units separated by soil layers that represents periods of minimal net sedimentation or minor hiatus at ~15 and ~ 45 m.

The lowermost OSL sample from ~42 m depth gives an age of 86 ± 7.4 ka, and by extrapolation the base of the core at 50 m would be over ~100 ka. Sinha et al. (2007) reported luminescence chronology of this core based on etched K-feldspar dating. Four samples from depths 11.6, 21.5, 31.9 and 41.9 m were dated which constrained the total time represented by this core to ~100 ka. The surface sediment is assumed to be of contemporary age, consistent with ^{14}C age of 5.4 ± 0.4 ka for carbonate nodules separated from a depth of 2.3 m in this study. The available chronology of this core suggests a variable rate of sedimentation. These ages yield roughly similar sedimentation rates (0.41 ± 0.03 m/ka) for the depth intervals 0 to 11.6 m, 21.5 to 31.9 m and 31.9 to 41.9 m. The sedimentation rate for the interval 11.6 to 21.5 m is relatively high, 1.2 ± 0.7 m/ka. The age model for the core was constructed using these data.

2. Analysis

Sediment samples were dried at about 50 ^{o}C for 2-3 days in an oven and about 50 grams of dried samples were powdered to ≤ 100 μm size using an agate mortar and pestle. Sr and Nd isotope measurements were made on the *silicate fraction* of sediments after decarbonating the bulk samples by leaching them with 0.6 N HCl at 80 ^{o}C for ~30 minutes with intermittent ultrasonic treatment. The decarbonated samples were ashed at ~ 600 ^{o}C to oxidize organic matter. ~100 mg of carbonate and organic matter free sediments were digested with HF-HNO_3 acids in the presence of ^{84}Sr and ^{150}Nd spikes.

Finally they were taken in 2N HCl and Sr and Nd were separated from the solution following reported ion exchange procedures (Richard et al., 1976; Alibert et al., 1983; Galy, 1999; Rai and Singh, 2007; Singh et al., 2008). Sr and Nd concentrations and their $^{87}Sr/^{86}Sr$ and $^{143}Nd/^{144}Nd$ were measured on Isoprobe-T Thermal Ionization Mass Spectrometer in static multi-collection mode. Mass fractionation corrections for Sr and Nd were made by normalizing $^{86}Sr/^{88}Sr$ to 0.1194 and $^{146}Nd/^{144}Nd$ to 0.7219. During the course of analyses, SRM987 Sr and JNdi-1 Nd standards were repeatedly measured, these yielded values of 0.710229±0.000014 (1σ, n = 85) for $^{86}Sr/^{88}Sr$ and 0.512102±0.000008 (1σ, n = 13) for $^{143}Nd/^{144}Nd$, well within their recommended values. Several Sr and Nd total procedural blanks were processed along with the samples. These blanks are several orders of magnitude lower than typical total Sr and Nd loads analysed and hence no corrections for blanks were made. The average uncertainty is ± 0.0001 for $^{87}Sr/^{86}Sr$ (n=3 pairs) and 0.3 ε units for Nd (n=2 pairs) based on repeat measurements of the same samples which are larger than analytical precision and can be explained in terms of sample heterogeneity.

3. Data Analysis

Sr, Nd concentrations in sediments and their isotope compositions are given in Table DR1. Both concentrations and isotope composition of these sediments vary significantly. Sr and Nd concentration varies from 49 to 225 and from 18 to 42 μg g^{-1} respectively, similar to their sources, the Higher Himalaya (HH) and the Lesser Himalaya (LH). Sr and Nd isotope composition range from 0.72701 to 0.76708 and from -14.4 to -16.6 respectively. The $^{87}Sr/^{86}Sr$ and $\varepsilon_{Nd}(0)$ of these sediments fall between the range defined by the lithologies of the Higher and the Lesser Himalaya. The Sr and Nd isotope composition of the rocks of the Higher and Lesser Himalaya are compiled by Singh et al. (2008) and given in Table DR2. The Higher Himalayan rocks are characterized by radiogenic Nd and lower $^{87}Sr/^{86}Sr$ whereas those of the Lesser Himalaya have very radiogenic Sr and less radiogenic Nd (Table DR2; Singh et al., 2008 and references therein). The core site of this study receives sediments brought by the Ganga or ancestor of the Ganga. These sediments are sourced from the Higher and Lesser Himalaya. Studies on the contemporary sediments indicate that ~70% of the sediments in the Ganga are derived from the Higher Himalaya (Singh et al., 2008; Campbell et al., 2005). The Higher Himalaya has remained the main source of sediment to the Bay of Bengal since the Miocene (France-Lanord et al., 1993).

Tectonics and climate are two major factors controlling the erosion in the Himalaya and at shorter time scale such as in this study, impact of variation in tectonics can be negligible on the erosion variability if any. Climate has changed significantly over the time period considered in this study and can affect the erosion pattern over the Himalaya. Any variability in the erosion pattern over Himalaya will be the best recorded in the Ganga Plain, particularly at the core site as it receives sediments only from the Himalaya, i.e. the from the Higher and Lesser Himalaya. Sr and Nd isotope composition of the sediments deposited at the core site of this study can be used to track any variability in the erosion pattern over HH and LH as their isotope compositions are quite distinct provided that the sediments deposited in the plain preserve the isotope characteristics of their sources. Several studies have been carried out using Sr and Nd isotope composition of the contemporary sediments (Singh and France-Lanord, 2002;

Singh et al., 2008) and sediments deposited in the Bay of Bengal and in the Indus delta (Colin et al., 1999; Ahmad et al., 2005; Clift et al., 2008) to track their sources. It has been shown (Singh et al., 2008) that the isotopic composition of the contemporary sediments of the Ganga in the plain represents their sources and weathering and transport do not alter their isotopic signature. Similar to the coarser fraction, even the finer size fraction of the sediments represents their source isotope composition ruling out any impact of weathering and transport on their isotope composition (Galy and France-Lanord, 2001; Singh and France-Lanord et al., 2002; Singh et al., 2008) in the Ganga basin. However concentrations of Sr and Nd shows variability arising due to size sorting and chemical weathering and it is difficult to use the concentration alone to track their sources.

As discussed earlier the sediments analysed in this study are mostly flood plain deposits and in general they are dominated by mud and silt. Both Sr and Nd isotope composition of these sediments do not show any correlation with their respective concentrations (Fig DR2) or with Al content of these sediments (Fig. DR3), indicating very little affect of alteration on these sediments by weathering and transport processes. Further, in the scatter plot of $^{87}Sr/^{86}Sr$ vs ε_{Nd} (Fig. DR4), they show a trend similar to those observed for contemporary sediments (Singh et al., 2008) and can be explained by mixing between the sediments derived from the Higher and Lesser Himalaya. ε_{Nd} of these sediments decrease with increasing $^{87}Sr/^{86}Sr$, indicating varying proportion of the sediments from HH and LH. The observed scatter in the plot is due to the scatter in the source rocks of HH and LH (Table DR2). In all these plots, two samples seems to show anomalous behaviour. The one sample collected from depth 14.46 m, has the highest Sr concentration, 225 μg g^{-1} and the lowest $^{87}Sr/^{86}Sr$, 0.727. There could be several reasons for this sample. It could be either due to the source variability with higher proportion from the Tethyan Sedimentary Sequence of HH or could be due to the weathering effect. This particular sample has been collected from a section which shows sign of pedogenesis (Fig. DR1) which can alter the Sr isotope record but not the Nd. Other anomalous sample is from depth 34.09 with higher $^{87}Sr/^{86}Sr$ and not so lower ε_{Nd}. This can also be explained by source variability. Further, this sample is collected from a section of the core with discrete flood deposit (Fig. DR1) and may represent the sediments derived from a small basin characterized by Sr and Nd isotope composition similar to those observed for this sample. Despite their anomalous behaviour, the Sr and Nd isotope composition of these two sediments are still defined by the mixing between HH and LH. The interpretation of this study remains the same even if these two anomalous samples are not considered. Variations in the concentrations of Sr and Nd in these sediments could be partly due to source variability and, in part, could arise due to size sorting/quartz dilution. Further, available results on Sr and Nd concentrations of rocks of HH and LH display similar range and therefore cannot be used for tracking their varying contributions.

References

Ahmad, S. M., Babu, G. A., Padmakumari, V. M., Dayal, A. M., Sukhija, B. S. and Nagabhushanam, P., 2005, Sr, Nd isotopic evidence of terrigenous flux variations in the Bay of Bengal: Implications of monsoons during the last ~34,000 years: Geophysical Research Letters, v. 32, L22711.

Alibert, C., A. Michard, and F. Albarede, 1983, The transition from alkali basalts to kimberlites: Isotope and trace element evidence from melilitites: Contributions to Mineralogy and Petrology, v. 82, p. 176-186.

Campbell, I.H., Reiners, P.W., Allen, C.M., Nicolescu, S., and Upadhyay, R., 2005, He-Pb double dating of detrital zircons from the Ganges and Indus Rivers: Implication for quantifying sediment recycling and provenance studies: Earth and Planetary Science Letters, v. 237, p. 402-432.

Clift P.D., Giosan, L., Blusztajn, J., Campbell, I.H., Allen, C., Pringle, M., Tabrez, A.R., Danish, M., Rabbani, M.M., Alizai, A., Carter A., and Lückge A., 2008, Holocene erosion of the Lesser Himalaya triggered by intensified summer monsoon, Geology, v. 36, p. 79–82.

Colin C., Turpin, L., Bertaux, J., Desprairies, A. and Kissel, C., 1999, Erosional history of the Himalayan and Burman ranges during the last two glacial–interglacial cycles: Earth and Planetary Science Letters, v. 171, p. 647–660.

France-Lanord, C., Derry, L., and Michard, A., 1993, Evolution of the Himalaya since Miocene time: Isotopic and sedimentologic evidence from the Bengal Fan, *in* Treloar, P.J., and Searle, M., eds., Himalayan Tectonics: Geological Society [London] Special Publication 74, p. 603–621.

Galy, A., 1999, Etude ge´ochimique de l'e´rosion actuelle de la chaine himalayenne [Ph.D. thesis]: Nancy, Institut National Polytechnique de Lorraine, 466 p.

Galy, A., and France-Lanord, C., 2001, Higher erosion rates in the Himalaya: Geochemical constraints on riverine fluxes: Geology, v. 29, p. 23–26.

Rai, S.K., and Singh, S.K., 2007, Temporal variation in Sr and $^{87}Sr/^{86}Sr$ of the Brahmaputra: Implications for annual for fluxes and tracking flash floods through chemical and isotope composition: Geochemistry Geophysics Geosystems, v. 8, Q08008, doi: 10.1029/2007GC001610.

Richard, P., Shimizu, N., and Allegre, C.J., 1976, $^{143}Nd/^{144}Nd$, a natural tracer: an application to oceanic basalts: Earth and Planetary Science Letters, v. 31, p. 269-278.

Singh, S.K, Rai, S.K., and Krishnaswami S., 2008, Sr and Nd isotopes in river sediments from the Ganga Basin: Sediment Provenance and Hotspots of Physical Erosion: Journal of Geophysical Research, v. 113, F03006, doi:10.1029/2007JF000909.

Singh, S.K., and C. France-Lanord, 2002, Tracing the distribution of erosion in the Brahmaputra watershed from isotopic compositions of stream sediments: Earth and Planetary Science Letters, v. 202, p. 645-662.

Sinha, R., Bhattacharjee, P.S., Sangode, S.J., Gibling, M.R., Tandon, S.K., Jain M., and Godfrey-Smith D., 2007, Valley and interfluve sediments in the Southern Ganga Plains, India: Exploring facies and magnetic signatures: Sedimentary Geology, v. 201, p. 386–411.

Figure Caption

Fig. DR1: Litho-stratigraphy of the core analysed in this study. The entire core represents flood plain deposit with almost continuous deposition. The sediments of this core are dominated by mud and silt intersperse with intermittent carbonate nodules locally termed as "kankar".

Fig. DR2: Scatter plot of Sr and Nd isotope composition with their concentrations in the sediments. Absence of any correlation among them rules out possibility of alteration of their isotope composition due to size sorting or weathering and hence they represent their source composition.

Fig. DR3: Scatter plot of $^{87}Sr/^{86}Sr$ and ε_{Nd} with their Al content. Sr and Nd isotope composition of the sediments are not correlated with their Al content, indicating very little impact of transport and weathering on the isotope composition of the sediments, if any.

Fig. DR4: $^{87}Sr/^{86}Sr$ vs ε_{Nd}. Sr and Nd isotopes of these sediments are result of the mixing between the sediments derived from the Higher and Lesser Himalaya. Two anomalous samples (encircled) could be due to the large variability in the sources or related to the pedogensis and discrete flood events as discussed in the text.

Table DR1: Sr, Nd isotope composition of sediments

Sample	Depth (m)	[Sr] (μg/g)	$^{87}Sr/^{86}Sr$	[Nd] (μg/g)	$^{143}Nd/^{144}Nd$	ε_{Nd}
IITK0.5	0.50	88	0.74756	24	0.511842	-15.5
IITK1.4	1.40	84	0.74548	19	0.511902	-14.4
IITK2.55	2.50	72	0.75069	22	0.511859	-15.2
IITK3.05	3.05	98	0.74196	22	0.511871	-15.0
IITK5.33	5.33	80	0.76027	21	0.511786	-16.6
IITK6.55	6.55	77	0.76510	23	0.511786	-16.6
IITK9.06	9.06	49	0.75008	23	0.511816	-16.0
IITK10.30	10.30	97	0.75096	23	0.511825	-15.9
IITK11.14	11.14	114	0.75148	32	0.511811	-16.1
IITK11.88	11.88	100	0.75624	22	0.511812	-16.1
IITK14.46	14.46	225	0.72701	18	0.511846	-15.5
IITK15.79	15.79	122	0.74732	26	0.511805	-16.3
IITK17.37	17.37	122	0.75214	42	0.511791	-16.5
IITK20.46	20.46	141	0.73447	26	0.511857	-15.2
IITK21.10	21.10	101	0.73998	23	0.511857	-15.2
IITK25.72	25.72	80	0.73580	22	0.511902	-14.4
IITK28.46	28.46	88	0.74045	31	0.511868	-15.0
IITK31.52	31.52	88	0.74504	27	0.511866	-15.1
IITK34.09	34.09	126	0.76708	28	0.511862	-15.1
IITK35.16	35.16	97	0.75804	25	0.511822	-15.9
IITK38.55	38.55	106	0.73824	31	0.511858	-15.2
IITK41.23	41.23	105	0.74583	21	0.511821	-15.9
IITK43.72	43.72	128	0.73625	29	0.511863	-15.1
IITK45.4	45.40	91	0.74002	22	0.511871	-14.8
IITK46.0	46.00	109	0.73646	28	0.511847	-15.4
IITK47.1	47.10	107	0.73687	26	0.511857	-15.2
IITK51.0	51.00	97	0.74042	21	0.511813	-16.1

Table DR2: $^{87}Sr/^{86}Sr$ and ε_{Nd} of various litho-units of the Ganga System[a]

Lithology	**$^{87}Sr/^{86}Sr$**		**ε_{Nd}**	
	Range	**Typical**	**Range**	**Typical**
<u>Higher Himalaya</u>				
TSS	0.71-0.73	0.727 ± 0.012	-15 – -12	-13
HHC	0.73-0.79	0.76 ± 0.03	-16.4 – -13.6	-15 ± 1.4
<u>Lesser Himalaya</u>				
LH	0.72-0.94	0.85 ± 0.09	-25.3 – -23.5	-24.4 ± 0.9
<u>Siwaliks</u>	0.72-0.76	0.738 ± 0.018	-19 – -15	-17.2 ± 1.2

[a]Singh et al., 2008 and references therein; TSS:Tethyan Sedimentary Sequence; HHC: Higher Himalaya Crystallines: LH: Lesser Himalaya

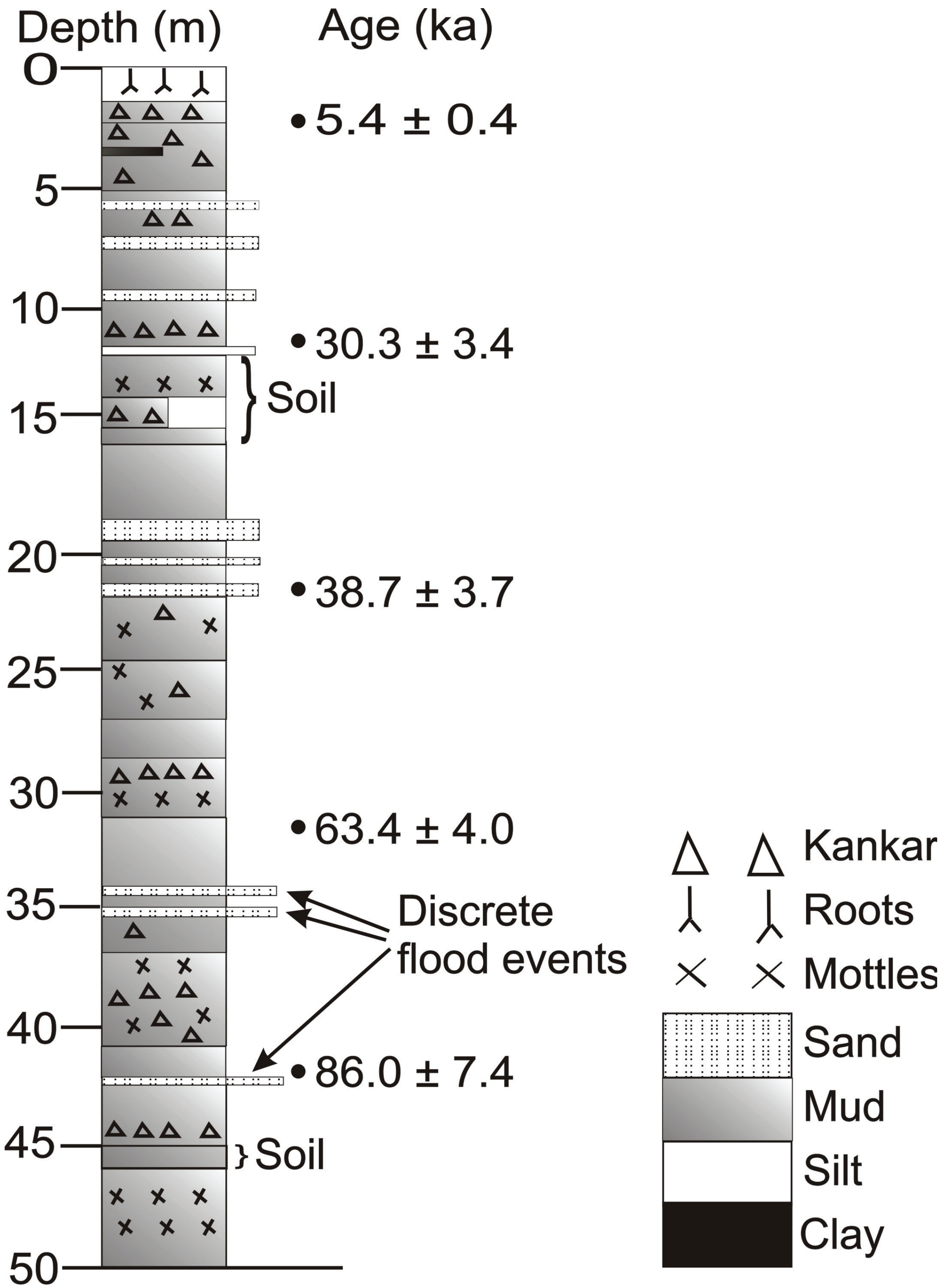

Depth (m)
Age (ka)
0
5
10
15
20
25
30
35
40
45
50
5.4 ± 0.4
30.3 ± 3.4
Soil
38.7 ± 3.7
63.4 ± 4.0
Discrete
flood events
86.0 ± 7.4
Soil
Kankar
Roots
Mottles
Sand
Mud
Silt
Clay

Fig. DR1

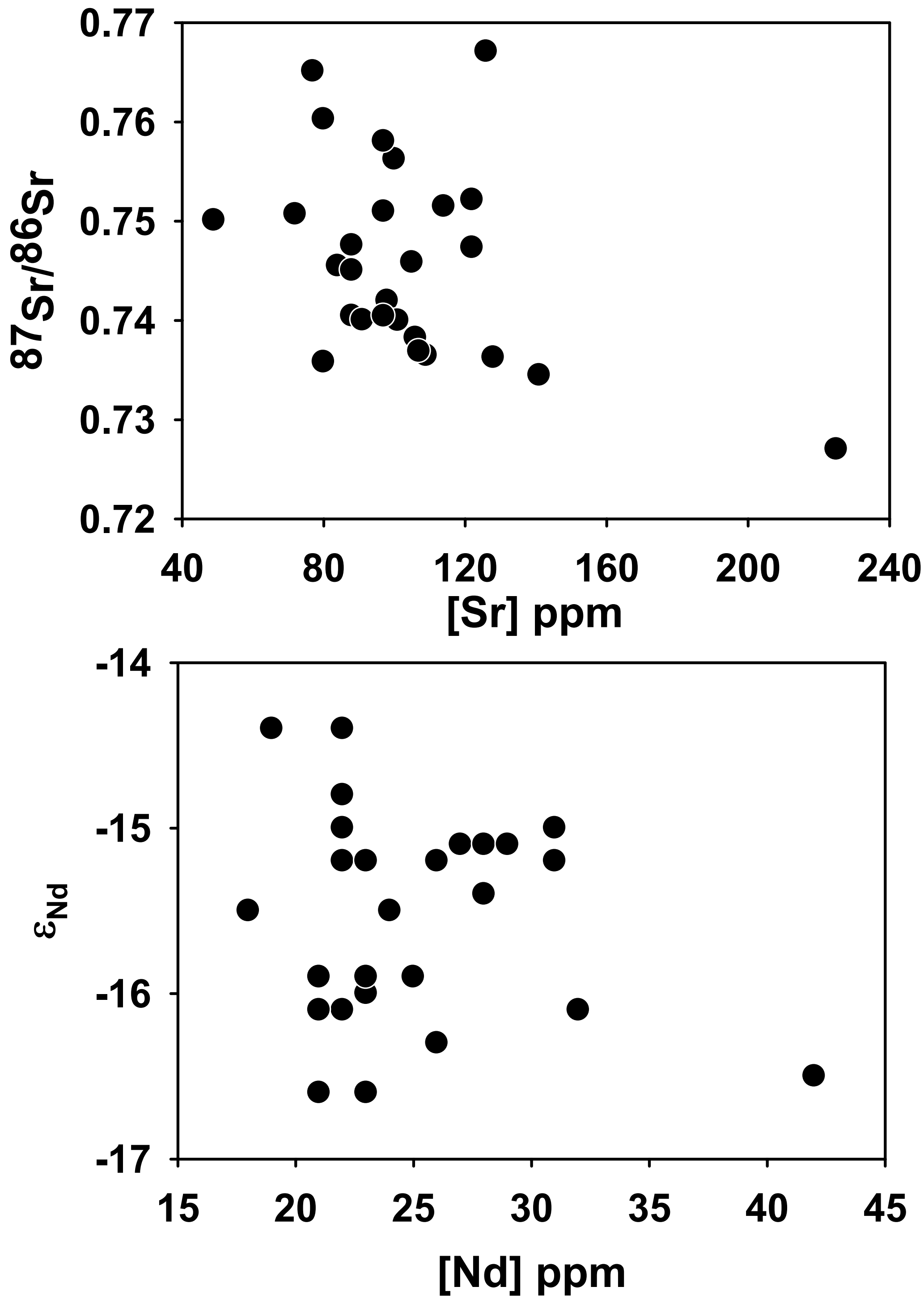

0.77
0.76
0.75
0.74
0.73
0.72
87Sr/86Sr
40
80
120
160
200
240
[Sr] ppm
-14
-15
-16
-17
εNd
15
20
25
30
35
40
45
[Nd] ppm

Fig. DR2

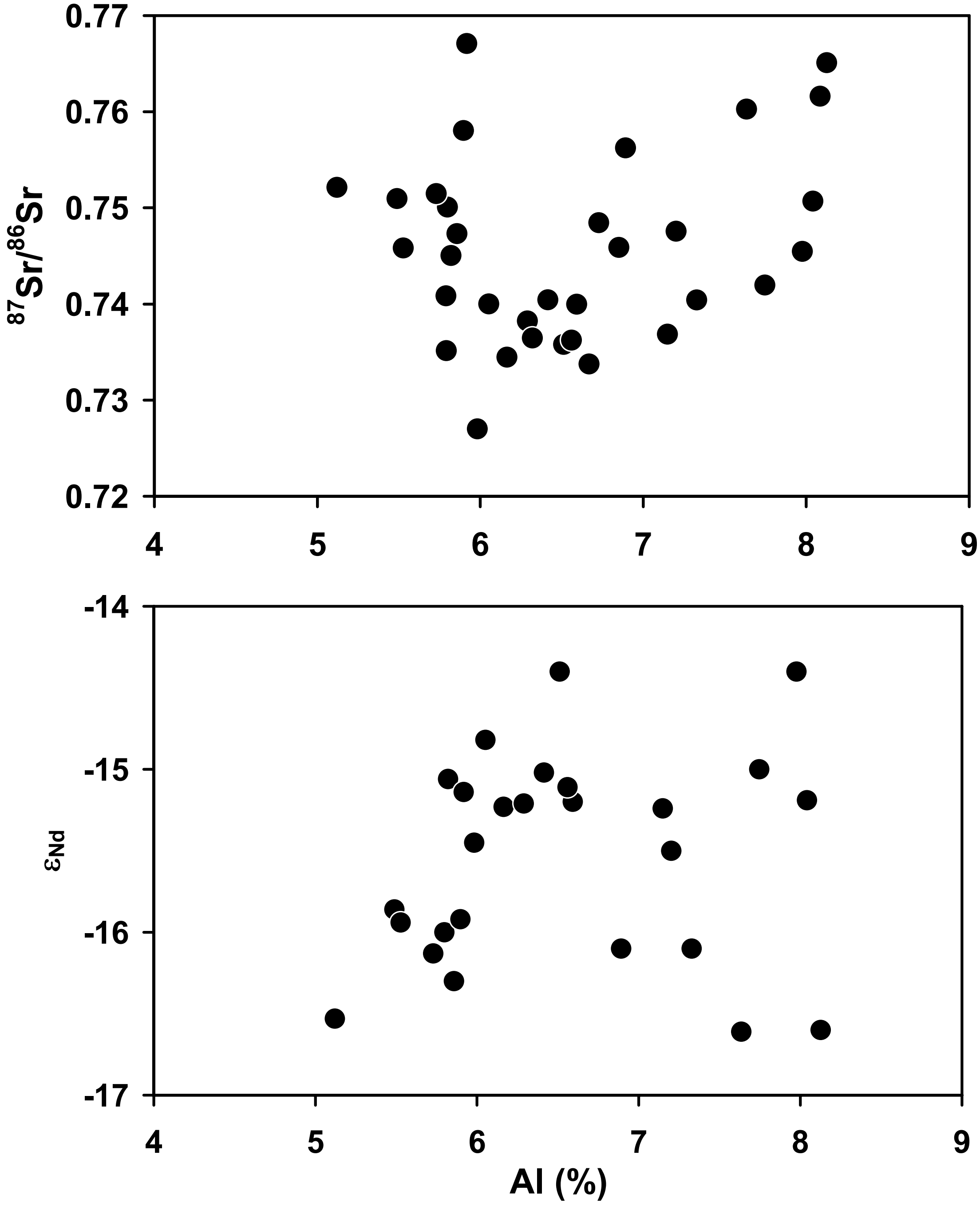
0.77
0.76
0.75
0.74
0.73
0.72
87Sr/86Sr
4
5
6
7
8
9
-14
-15
-16
-17
εNd
4
5
6
7
8
9
Al (%)

Fig. DR3

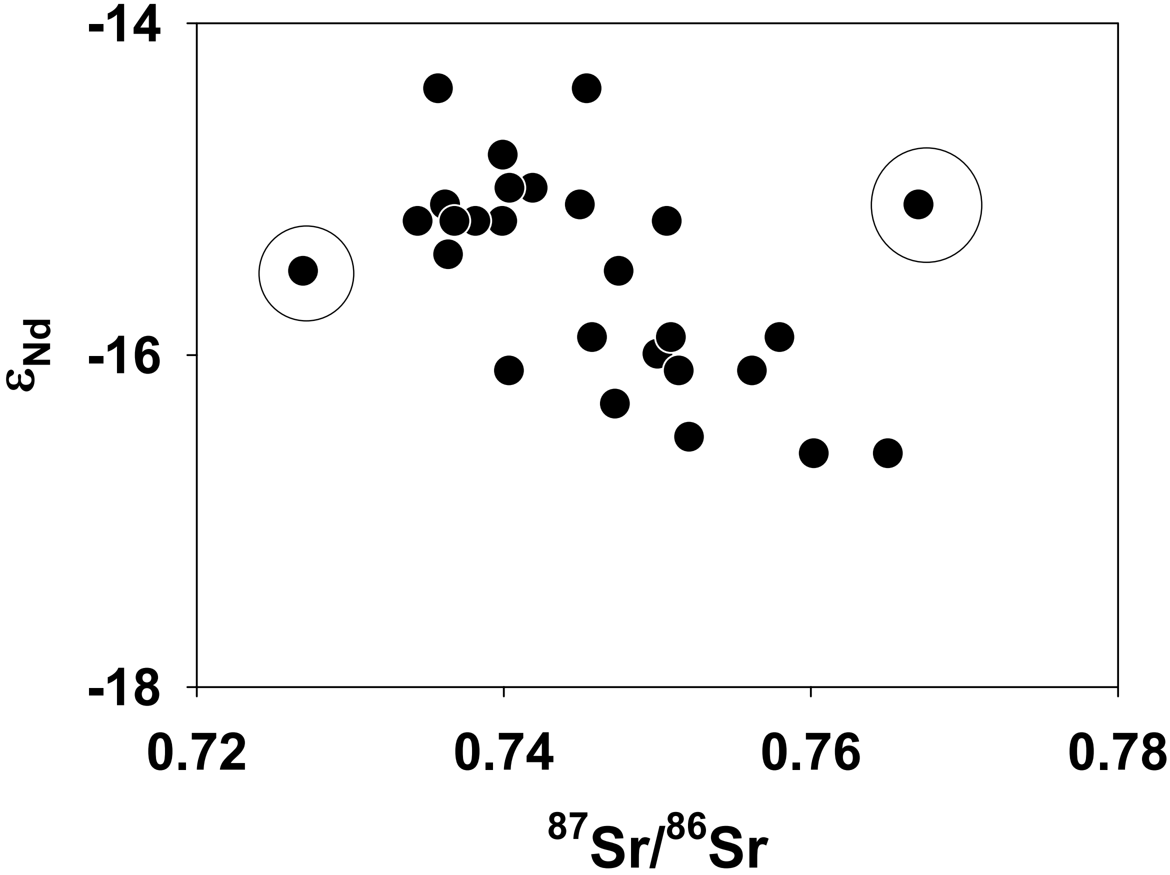

Fig. DR4